

# 000 001 002 003 004 005 006 007 008 009 010 011 012 013 014 015 016 017 018 019 020 021 022 023 024 025 026 027 028 029 030 031 032 033 034 035 036 037 038 039 040 041 042 043 044 045 046 047 048 049 050 051 052 053 LEARNING FAIR GRAPH REPRESENTATIONS WITH MULTI-VIEW INFORMATION BOTTLENECK

Anonymous authors

Paper under double-blind review

## ABSTRACT

Graph neural networks (GNNs) excel on relational data by passing messages over node features and structure, but they can amplify training data biases, propagating discriminatory attributes and structural imbalances into unfair outcomes. Many fairness methods treat bias as a single source, ignoring distinct attribute and structural effects and leading to suboptimal fairness and utility trade-offs. To overcome this challenge, we propose FairMIB, a Multi-view information bottleneck framework designed to decompose graphs into feature, structural, and Diffusion Views for mitigating **complex biases** in GNNs. In particular, the proposed FairMIB employs contrastive learning to maximize cross-view mutual information for bias-free representation learning. It further integrates multi-perspective conditional information bottleneck objectives to balance task utility and fairness by minimizing mutual information with sensitive attributes. Additionally, FairMIB introduces an inverse probability-weighted (IPW) adjacency correction in the Diffusion View, which reduces the spread of bias propagation during message passing. Experiments on five real-world benchmark datasets demonstrate that FairMIB achieves state-of-the-art performance across both utility and fairness metrics.

## 1 INTRODUCTION

Graph Neural Networks (GNNs) represent a pivotal advancement in machine learning, offering a powerful paradigm for modeling complex relational data Wu et al. (2020b). Through a message-passing mechanism, GNNs iteratively aggregate information from a node and its neighbors, effectively capturing both node attributes and the graph's structural dependencies Mo et al. (2025). This capability to learn from intricate patterns has established GNNs as indispensable tools in various high-stakes domains, such as recommender systems Amara et al. (2025), drug discovery Wang et al. (2025), and social network analysis Feng & Qian (2025). Across these applications, GNNs consistently deliver superior performance by exploiting the rich interplay between node features and network topology, ultimately leading to more accurate and scalable predictions Chen et al. (2025).

Nevertheless, in real-world applications, data are inherently imperfect Ju et al. (2024b); Zhan et al. (2026), with biases arising from sampling bias, selection bias, and labeling bias Guo et al. (2023); Li et al. (2024b). When trained on such data, GNNs inevitably internalize and even amplify these biases Dai & Wang (2021), leading to outputs that may exhibit discriminatory or unfair behaviors Agarwal et al. (2021). Such unfairness not only compromises the reliability and practical adoption of models but also poses broader societal risks, including the potential erosion of public trust in intelligent systems. For example, biases in risk assessment tools toward specific groups can lead to unfair sentencing and bail decisions Lowden (2018), while systemic biases in credit scoring models against certain regions may result in inequitable loan approvals Li et al. (2024a). Consequently, fairness has emerged as a critical challenge that must be addressed to ensure the trustworthy deployment of Graph Convolutional Networks (GCNs) Zhang et al. (2024c).

Existing studies on fairness in GNNs generally fall into two categories: data-level methods Zhang et al. (2024a); Agarwal et al. (2021) and model-level methods Yang et al. (2024); Lee et al. (2025). The first category corrects biases at the data level through pre-processing techniques that adjust the data distribution, re-balance underrepresented groups, or modify node features and graph structures before training. By addressing bias at the source, these methods aim to mitigate its propagation during model learning. For example, FairGB Li et al. (2024b) achieves re-balancing by introducing

054 counterfactual node mixup and contribution alignment loss, while FG-SMOTE Wang et al. (2024)  
 055 creates synthetic nodes for underrepresented groups, assigns sensitive attributes proportionally, and  
 056 applies fair link prediction to generate non-discriminatory connections, thereby correcting both dis-  
 057 tributional and structural biases. Model-level approaches, on the other hand, incorporate fairness  
 058 directly into the training process, typically by embedding fairness as a regularization term or con-  
 059 straint within the objective function. These methods aim to restrict the leakage of sensitive infor-  
 060 mation, ensuring that learned representations **remain predictive** while minimizing dependence on  
 061 protected attributes. For example, FairVGNN Wang et al. (2022) enhances fairness by generating  
 062 fairness-aware Feature Views and applying adaptive weight pruning to mitigate sensitive attribute  
 063 leakage during feature propagation. Similarly, FairDLA Zhen et al. (2025) decouples task-related  
 064 and bias-related representations, then performs dual-layer alignment at both the sensitive attribute  
 065 group level and the task subgroup level to enhance fairness.  
 066

066 Model-based methods generally learn a single node representation where attribute, structural, and  
 067 propagation biases are intertwined, making it difficult to separate them from task-relevant features  
 068 and leaving residual sensitive information Zhu et al. (2024). Data-level pre-processing methods can  
 069 partially alleviate data imbalance Wang et al. (2024), but often treat distributional skew in isolation,  
 070 overlooking how sensitive information propagates and entangles during message passing Yang et al.  
 071 (2024). These methods often assume static and accurate graph structures and features, overlooking  
 072 noise, missing data, and outliers, which cause models to retain latent bias signals and result in in-  
 073 complete debiasing and fairness gaps Zhou et al. (2020); Li et al. (2024b). Model-based methods  
 074 typically rely on a single, entangled node representation that conflates bias signals from attributes,  
 075 structure, and propagation, leading to incomplete debiasing and residual sensitive information Zhu  
 076 et al. (2024). Such entanglement makes it difficult to disentangle the sources of bias, potentially  
 077 suppressing task-relevant features while retaining sensitive ones. Moreover, as bias accumulates  
 078 through multi-layer message passing and representation updates, residual sensitive attributes may  
 079 still be encoded in the latent space, and fairness constraints alone are often insufficient to prevent  
 080 systemic bias in downstream tasks Zhen et al. (2025). Furthermore, existing studies largely over-  
 081 look the issue of cross-view leakage, where biases from attribute-level, structural, and propagation  
 082 sources interact in complex ways, further amplifying unfair outcomes Lee et al. (2025).  
 083

083 To address these limitations, we propose a novel Multi-view Information Bottleneck framework for  
 084 Fair GNNs (FairMIB). FairMIB decomposes the graph into distinct informational views: *a Feature*  
 085 *View* derived from node attributes, *a Structural View* capturing the pure graph topology, and *a Diffusion*  
 086 *View* that models high-order neighborhood information. We employ contrastive learning  
 087 to maximize mutual information across these views, encouraging the model to learn representa-  
 088 tions that are invariant to view-specific noise and biases. Concurrently, we integrate the Information  
 089 Bottleneck (IB) principle as a fairness-aware objective. This objective simultaneously aims to max-  
 090 imize the mutual information between the learned representations and task labels while minimizing  
 091 the mutual information with sensitive attributes, thereby achieving a principled trade-off between  
 092 utility and fairness. Our contributions are as follows:  
 093

- 094 • We propose FairMIB, a novel Multi-view learning framework, designed to decouple and  
 095 mitigate mixed biases stemming from node attributes and graph structure. The framework  
 096 decomposes graph data into three independent views: features, structure, and diffusion. It  
 097 then learns robust node representations by maximizing consistency across the three views.  
 098
- 099 • We optimize task performance while introducing an IPW based feature matrix correction  
 100 method in the Diffusion View to block the amplification of sensitive attributes bias during  
 101 message propagation.  
 102
- 103 • We perform extensive experiments on five real-world datasets, demonstrating that FairMIB  
 104 outperforms state-of-the-art baselines in terms of fairness, utility, and stability.  
 105

## 106 2 RELATED WORK

107 In this section, we briefly review related work, with further details provided in Appendix A. Recent  
 108 fairness methods for GNNs are typically categorized into pre-processing Rahman et al. (2019); Dong  
 109 et al. (2022); Li et al. (2024b); Wang et al. (2024), in-processing Dai & Wang (2021); Wang et al.  
 110 (2022); Agarwal et al. (2021); Yang et al. (2024), and post-processing Lee et al. (2025). These  
 111 recent works include EDITS Dong et al. (2022) which reweights attributes and perturbs structure  
 112

108 for debiasing, FairGB Li et al. (2024b) which uses resampling and causal contrastive generation  
 109 to neutralize training views, FairVGNN Wang et al. (2022) which learns channel masks to reduce  
 110 dependence on sensitive features, NIFTY Agarwal et al. (2021) which employs adversarial and  
 111 counterfactual augmentations to stabilize embeddings, FairSIN Yang et al. (2024) which injects  
 112 fairness-promoting features from heterogeneous neighbors before propagation, FairSAD Zhu et al.  
 113 (2024) which disentangles sensitive factors and applies channel-wise masking, and DAB-GNN Lee  
 114 et al. (2025) which disentangles attribute and structural bias.

115 The IB aims to identify a minimal sufficient representation that compresses input data while retaining  
 116 critical information for subsequent tasks Kawaguchi et al. (2023). This principle has been extended  
 117 to graph learning through the Graph Information Bottleneck (GIB) model Wu et al. (2020a), which  
 118 compresses both node features and structural information. In fair graph representation learning, IB  
 119 shows potential by balancing utility and fairness, such as GRAFair Zhang et al. (2025), which uses  
 120 a variational graph autoencoder to ensure stable optimization. Recent efforts, such as FDGIB Zheng  
 121 et al. (2024), combines IB with disentanglement and counterfactual augmentation to decompose  
 122 node representations into sensitive and non-sensitive subspaces. However, relying on single-view  
 123 processing is limiting, as graph bias is multi-source, and single representations may conflate signals,  
 124 leading to under-correction and residual leakage.

### 125 3 PRELIMINARIES

128 In this section, we introduce the notations for graph-structured data, followed by a description of  
 129 commonly used fairness metrics, and then discuss **Multi-view** information bottleneck and Multi-  
 130 view conditional information bottleneck (MCIB). More details are presented in Appendix B.

#### 131 3.1 NOTATIONS

133 We represent an attributed graph as  $\mathcal{G} = (\mathcal{V}, \mathcal{E}, \mathbf{X})$ , where  $\mathcal{V} = \{v_1, v_2, \dots, v_n\}$  is a set of  $n$  nodes,  
 134 and  $\mathcal{E} \subseteq \{(v_i, v_j) | v_i, v_j \in \mathcal{V}\}$  is a set of  $m$  edges. The graph's topology is described by the  
 135 adjacency matrix  $\mathbf{A} \in \{0, 1\}^{n \times n}$ , where  $A_{ij} = 1$  if an edge exists between node  $v_i$  and  $v_j$ , and  
 136 0 otherwise; this definition can be naturally extended to directed or weighted graphs. Each node  
 137 is associated with features, forming the node feature matrix  $\mathbf{X} = [\mathbf{x}_1, \dots, \mathbf{x}_n]^\top \in \mathbb{R}^{n \times d}$ , where  
 138  $\mathbf{x}_i \in \mathbb{R}^{1 \times d}$  is the  $d$ -dimensional feature vector for node  $v_i$ . In the context of fairness research,  
 139 we use a binary vector  $\mathbf{S} \in \{0, 1\}^n$  to represent the sensitive attributes (e.g., gender, race) of all  
 140 nodes, where  $s_i$  is the sensitive attribute value for node  $v_i$ , which is typically included in the original  
 141 feature vector  $\mathbf{x}_i$ . If two nodes  $v_u$  and  $v_v$  satisfy  $s_u = s_v$ , they belong to the same demographic  
 142 group. For the downstream node classification tasks, the ground-truth node labels are represented  
 143 by the label vector  $\mathbf{Y} \in \{0, 1\}^n$ , while the low-dimensional representations learned by the GNNs  
 144 form the matrix  $\mathbf{Z} \in \mathbb{R}^{n \times d'}$ , where  $d'$  is the embedding dimension.

#### 145 3.2 MULTI-VIEW INFORMATION BOTTLENECK

147 From a theoretical perspective, the effectiveness of MIB relies on the redundancy of information  
 148 across multiple views Cui et al. (2023); Federici et al. (2020). Different views (e.g.,  $\mathcal{G}_i$  and  $\mathcal{G}_j$ ) often  
 149 provide overlapping predictive information for the same labels  $\mathbf{Y}$ . In the context of graph data, we  
 150 formally define view redundancy as follows:

152 **Definition 1 (View Redundancy)** A view  $\mathcal{G}_i$  is considered redundant with respect to view  $\mathcal{G}_j$  for  
 153 predicting the target labels  $\mathbf{Y}$  if and only if the mutual information  $I(\mathbf{Y}; \mathcal{G}_i | \mathcal{G}_j) = 0$ . Intuitively, this  
 154 means that after observing  $\mathcal{G}_j$ ,  $\mathcal{G}_i$  adds no new information for predicting  $\mathbf{Y}$ .

155 Based on this, the essential objective of MIB is to identify a cross-view minimal sufficient statistic.  
 156 It aims to learn a highly compressed representation  $\mathbf{Z}$  that retains all task-relevant information across  
 157 the views, making redundant views unnecessary. An ideal, informationally sufficient representation  
 158  $\mathbf{Z}$  satisfies:

159 **Corollary 1 (Representation Sufficiency)** If  $\mathbf{Z}$  is a sufficient representation of the views  
 160  $\{\mathcal{G}_1, \dots, \mathcal{G}_V\}$ , its predictive power for  $\mathbf{Y}$  is equivalent to that of all views combined:

$$I(\mathbf{Z}; \mathbf{Y}) = I(\mathcal{G}_1, \dots, \mathcal{G}_V; \mathbf{Y}) \quad (1)$$

162 To achieve this, MIB formulates the learning process as the following optimization problem:  
 163

$$164 \min_{P(\mathbf{Z}|\mathcal{G}_1, \dots, \mathcal{G}_V)} \sum_{v=1}^V I(\mathbf{Z}; \mathcal{G}_v) - \lambda I(\mathbf{Z}; Y) \quad (2)$$

$$165$$

$$166$$

167 where  $I(\mathbf{Z}; \mathcal{G}_v)$  measures the mutual information between the fused representation  $\mathbf{Z}$  and a single  
 168 view  $\mathcal{G}_v$ , corresponding to the compression objective.  $I(\mathbf{Z}; Y)$  measures the mutual information  
 169 between  $\mathbf{Z}$  and the target labels  $Y$ , representing the relevance to be preserved. The hyperparameter  
 170  $\lambda$  balances the trade-off between compression and relevance. By solving this, MIB distills the most  
 171 critical and pure shared knowledge from multiple views for decision-making.  
 172

### 173 3.3 MULTI-VIEW CONDITIONAL INFORMATION BOTTLENECK (MCIB)

174 In this section, we introduce the Conditional Fairness Bottleneck (CFB) Gálvez et al. (2021) for fair  
 175 graph representation learning, and extend it in Multi-view settings. Given views  $\{\mathcal{G}_1, \dots, \mathcal{G}_V\}$ , we  
 176 learn a fair fused representation  $\mathbf{Z}$  via the mapping  $P(\mathbf{Z} | \mathcal{G}_1, \dots, \mathcal{G}_V)$  that is minimally sufficient  
 177 for the task while being disentangled from the sensitive attribute  $\mathbf{S}$ . The goal is to preserve the  
 178 amount of fair information about the label  $Y$  that is independent of  $\mathbf{S}$  above a threshold  $r$ . Formally,  
 179 the optimization objective of the Multi-view conditional information bottleneck (MCIB) can be  
 180 defined as:  
 181

$$182 \min_{P(\mathbf{Z}|\mathcal{G}_1, \dots, \mathcal{G}_V)} \left\{ I(\mathbf{S}; \mathbf{Z}) + \sum_{v=1}^V I(\mathcal{G}_v; \mathbf{Z} | \mathbf{S}, Y) \right\} \quad \text{s.t.} \quad I(Y; \mathbf{Z} | \mathbf{S}) \geq r$$

$$183$$

184 where  $I(\mathbf{S}; \mathbf{Z})$  constrains sensitive information leakage, while the conditional redundancy term  
 185  $\sum_v I(\mathcal{G}_v; \mathbf{Z} | \mathbf{S}, Y)$  eliminates view-specific information that becomes irrelevant once  $\mathbf{S}$  and  $Y$  are  
 186 observed. The constraint  $I(Y; \mathbf{Z} | \mathbf{S}) \geq r$  ensures sufficient task-relevant information is retained,  
 187 yielding a compact, fair representation that balances utility and fairness across multiple views.  
 188

## 189 4 METHODOLOGY

190 In this section, we present the details of the proposed FairMIB framework. An overview of the  
 191 framework is provided in Figure 1, which illustrates how it is designed to learn fair node represen-  
 192 tations from graph data.  
 193

### 194 4.1 MULTI-VIEW DISENTANGLEMENT

195 Bias in GNNs arises from three main sources: node attributes, graph structure, and the information  
 196 diffusion mechanism. FairMIB is designed to disentangle these intertwined factors by decomposing  
 197 them into three complementary views.  
 198

#### 200 4.1.1 DIFFUSION VIEW

201 The *Diffusion View* captures potential dynamic deviations that occur as information propagates  
 202 across the graph. To prevent sensitive attributes from introducing bias during this process, Fair-  
 203 MIB applies proactive intervention strategies (see Figure 5). Specifically, before propagation, we  
 204 use IPW Li et al. (2018) to adjust the node feature matrix. The propensity score  $e(i)$  represents the  
 205 probability that a node belongs to the sensitive group, given its features  $\mathbf{x}_i$ :  $e(i) = P(s = 1 | \mathbf{x}_i)$ .  
 206 Each node is then assigned a weight based on the IPW formulation:  
 207

$$208 w_i = \frac{s_i}{e(i)} + \frac{1 - s_i}{1 - e(i)} \quad (3)$$

$$209$$

$$210$$

211 These weights are used to construct a reweighted feature matrix  $W = \text{diag}(w_1, \dots, w_n)$ , which  
 212 produces the debiased feature matrix  $\mathbf{X}' = W\mathbf{X}$ . This reweighting balances the influence of nodes  
 213 from different sensitive groups within the feature space.  
 214

215 To model diffusion, we adopt the Personalized Propagation of Neural Predictions (APPNP) Klicpera  
 216 et al. (2019). A key advantage of APPNP is that it decouples feature transformation from propa-  
 217 gation, enabling efficient aggregation of multi-hop neighborhood information. The diffused feature  
 218

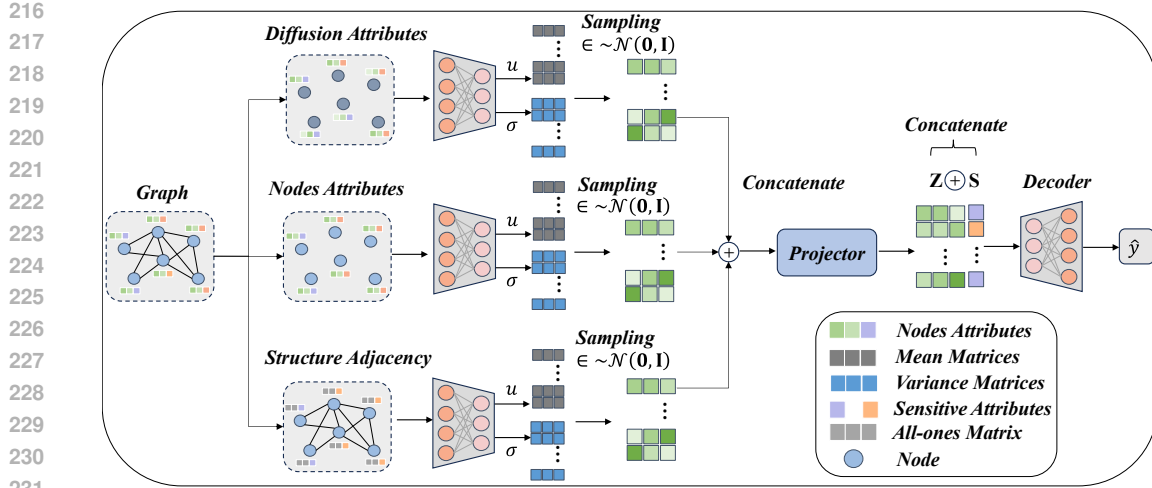


Figure 1: Overview of the proposed FairMIB framework. The model first disentangles the input graph into three complementary views: a **Diffusion View**, a **Feature View**, and a **Structural View**. Each view is encoded by a dedicated variational encoder to obtain a latent representation. These representations are then fused through a Projector, producing a fair representation that is concatenated with the sensitive attribute  $\mathbf{S}$  during training to guide the Decoder toward fair predictions.

matrix  $\mathbf{X}_{\text{diff}}$  is computed as:

$$\mathbf{X}_{\text{diff}} = \alpha \left( \mathbf{I} - (1 - \alpha) \tilde{\mathbf{A}} \right)^{-1} \mathbf{X}' \quad (4)$$

where  $\mathbf{X}'$  is the initial node feature matrix that is propagated along these pathways, and  $\alpha$  is the teleport probability that controls the balance between retaining initial features and aggregating neighborhood information.

Finally, the **Diffusion View** is defined as  $\mathcal{G}_{\text{diff}} = (\mathcal{V}, \mathbf{I}, \mathbf{X}_{\text{diff}})$ , representing a graph that contains only the debiased node attributes from the fair diffusion process, with structural information implicitly encoded in the features.

#### 4.1.2 FEATURE VIEW AND STRUCTURAL VIEW

The **Feature View** isolates the influence of the topological structure, focusing on potential biases in the intrinsic node attributes. It is defined as a graph without inter-node edges,  $\mathcal{G}_{\text{feat}} = (\mathcal{V}, \mathbf{I}, \mathbf{X})$ , where  $\mathbf{X} \in \mathbb{R}^{n \times d}$  is the node feature matrix and  $\mathbf{I}$  is the identity matrix, ensuring each node is connected only to itself. This view allows the encoder to learn information solely from the node attributes, isolating biases from structural factors like homophily.

In contrast, the **Structural View** is designed to completely isolate the influence of node attributes, focusing exclusively on the potential biases present within the graph's pure topological structure. It is defined as  $\mathcal{G}_{\text{struct}} = (\mathcal{V}, \mathbf{A}, \mathbf{1})$ , where  $\mathbf{A} \in \mathbb{R}^{n \times n}$  is the original adjacency matrix, and the node feature matrix is replaced by an all-ones matrix  $\mathbf{1} \in \mathbb{R}^{n \times d}$ . This approach forces the encoder to learn representations solely from connectivity patterns, thereby isolating biases that are introduced by correlations between the node features and sensitive attributes.

## 4.2 FAIR REPRESENTATION LEARNING VIA MCIB

Since the mutual information terms are intractable to optimize directly, we employ variational approximation to derive a tractable objective. For the compression term,  $I(\{\mathcal{G}_{\text{view}}\}; \mathbf{Z})$ , we use the KL-divergence as its upper bound:

$$I(\{\mathcal{G}_{\text{view}}\}; \mathbf{Z}) \leq \sum_{\text{view}} D_{\text{KL}}(p_{\theta_{\text{view}}}(\mathbf{Z}_{\text{view}} | \mathcal{G}_{\text{view}}) \| q(\mathbf{Z}_{\text{view}})) \quad (5)$$

where  $p_{\theta_{\text{view}}}$  is the posterior distribution defined by a view-specific encoder with parameters  $\theta_{\text{view}}$ , and  $q(\mathbf{Z}_{\text{view}})$  is a prior distribution, typically set to a standard normal distribution  $\mathcal{N}(0, \mathbf{I})$ .

270 For the fair prediction term,  $I(Y; \mathbf{Z}|\mathbf{S})$ , we derive its lower bound:  
 271

$$272 \quad I(Y; \mathbf{Z}|\mathbf{S}) \geq \mathbb{E}_{p(Y, \mathbf{Z}, \mathbf{S})} [\log p_\phi(Y|\mathbf{Z}, \mathbf{S})] \quad (6)$$

273 where  $p_\phi$  is the predictive distribution defined by a decoder with parameters  $\phi$ .  
 274

275 Combining these bounds, our loss function  $\mathcal{L}_{\text{MCFB}}$  can be expressed as:  
 276

$$277 \quad \mathcal{L}_{\text{MCFB}} = \sum_{\text{view}} D_{\text{KL}}(p_{\theta_{\text{view}}}(\mathbf{Z}_{\text{view}} | \mathcal{G}_{\text{view}}) \| q(\mathbf{Z}_{\text{view}})) - \gamma \mathbb{E}_{p(Y, \mathbf{Z}, \mathbf{S})} [\log p_\phi(Y | \mathbf{Z}, \mathbf{S})] \quad (7)$$

279 Minimizing this loss function is equivalent to maximizing the Evidence Lower Bound (ELBO),  
 280 which allows us to achieve our optimization objective in a stable, non-adversarial manner.  
 281

#### 282 4.3 MULTI-VIEW CONSISTENCY CONSTRAINT

284 Although our framework disentangles sources of bias and debiases fused view with a conditional  
 285 information bottleneck, all three views originate from the same graph, so their fair representations  
 286 should share a unified task-relevant core in the latent space. To enforce this, we add a Multi-view  
 287 consistency constraint via contrastive learning Ju et al. (2024a), pulling together a node’s debiased  
 288 representations from different views as positives and pushing apart different nodes as negatives,  
 289 which drives view-specific encoders to learn a shared, robust, and sensitive invariant semantic space.  
 290

291 We implement this constraint using the InfoNCE loss Rusak et al. (2025). For a node  $v_i$ , let its latent  
 292 representations from the feature, structural, and Diffusion Views be  $\mathbf{z}_{i,\text{feat}}$ ,  $\mathbf{z}_{i,\text{struct}}$ , and  $\mathbf{z}_{i,\text{diff}}$ . We  
 293 can select the representations from any two views (e.g., the feature and Structural Views) to form a  
 294 positive pair  $(\mathbf{z}_{i,\text{feat}}, \mathbf{z}_{i,\text{struct}})$ . The contrastive loss for this pair is:  
 295

$$296 \quad \mathcal{L}_{\text{con}}(\mathbf{z}_{i,\text{feat}}, \mathbf{z}_{i,\text{struct}}) = -\log \frac{\exp(\text{sim}(\mathbf{z}_{i,\text{feat}}, \mathbf{z}_{i,\text{struct}})/\tau)}{\sum_{j=1}^N \exp(\text{sim}(\mathbf{z}_{i,\text{feat}}, \mathbf{z}_{j,\text{struct}})/\tau)} \quad (8)$$

297 where  $\text{sim}(\mathbf{u}, \mathbf{v})$  is a function that measures the similarity between two vectors, typically cosine  
 298 similarity. The term  $\tau$  is a temperature hyperparameter that adjusts the distribution of the similarity  
 299 scores, and  $N$  is the total number of nodes in the batch. The denominator includes the similarity  
 300 scores between the anchor  $\mathbf{z}_{i,\text{feat}}$  and one positive sample  $\mathbf{z}_{i,\text{struct}}$ , as well as  $N - 1$  negative samples  
 301  $\mathbf{z}_{j,\text{struct}}$  for  $j \neq i$ .  
 302

303 We apply this loss function to all pairwise combinations of the views and average the result over all  
 304 nodes to obtain the final Multi-view consistency loss  $\mathcal{L}_{\text{con}}$ :  
 305

$$306 \quad \mathcal{L}_{\text{con}} = \frac{1}{N} \sum_{i=1}^N \left( \mathcal{L}_{\text{con}}(\mathbf{z}_{i,\text{feat}}, \mathbf{z}_{i,\text{struct}}) + \mathcal{L}_{\text{con}}(\mathbf{z}_{i,\text{feat}}, \mathbf{z}_{i,\text{diff}}) + \mathcal{L}_{\text{con}}(\mathbf{z}_{i,\text{struct}}, \mathbf{z}_{i,\text{diff}}) \right) \quad (9)$$

308 By minimizing  $\mathcal{L}_{\text{con}}$ , the model encourages the representations of the same node across different  
 309 views to be close, while separating representations of different nodes. This promotes the learning of  
 310 a well-structured, semantically consistent, and fair representation space.  
 311

#### 312 4.4 THE OBJECTIVE FUNCTION OF FAIRMIB METHOD

313 During training, we concatenate the projected representation  $\mathbf{Z}_{\text{proj}}$  with the ground-truth sensitive  
 314 attributes  $\mathbf{S}$ . This combined vector is then fed into a decoder,  $h_\phi$ , implemented as a multilayer  
 315 perceptron (MLP), to make the final node classification predictions  $\hat{\mathbf{y}}$ :  
 316

$$317 \quad \hat{\mathbf{y}} = h_\phi([\mathbf{Z}_{\text{proj}} \| \mathbf{S}]) \quad (10)$$

318 This architectural design compels the encoders and the projector to learn information that remains  
 319 useful for predicting  $Y$  even when  $\mathbf{S}$  is provided. Consequently, it encourages the model to ignore  
 320 spurious correlations that are associated with  $\mathbf{S}$  but are irrelevant to the prediction task. The standard  
 321 cross-entropy loss for the node classification task is defined as:  
 322

$$323 \quad \mathcal{L}_{\text{task}} = -\frac{1}{|\mathcal{V}|} \sum_{v \in \mathcal{V}} (y \log \hat{y} + (1 - y) \log(1 - \hat{y})) \quad (11)$$

324 The overall training loss function of our FairMIB combines three main components: the task loss,  
 325 the Multi-view conditional fairness bottleneck loss, and the Multi-view consistency loss. The total  
 326 loss is given by:

$$\mathcal{L}_{\text{total}} = \mathcal{L}_{\text{task}} + \lambda_{\text{KL}} \mathcal{L}_{\text{MCFB}} + \lambda_{\text{con}} \mathcal{L}_{\text{con}} \quad (12)$$

328 where  $\lambda_{\text{KL}}$  and  $\lambda_{\text{con}}$  are hyperparameters that balance the objectives of information compression and  
 329 cross-view consistency, respectively.  
 330

## 331 5 EXPERIMENTS

334 In this section, we evaluate the proposed FairMIB framework on five real-world graph datasets.  
 335 More details of datasets, compared methods, experimental settings, experimental results and analysis  
 336 are provided in Appendix D due to page limitation. Our evaluation is guided by the following  
 337 research questions:

338 **RQ1:** Does FairMIB achieve superior performance in both utility and fairness compared with state-  
 339 of-the-art baselines? **RQ2:** What is the contribution of each component within the proposed Fair-  
 340 MIB framework to overall performance? **RQ3:** How do different informational views (feature,  
 341 structural, diffusion) affect representation quality and fairness outcomes? **RQ4:** How sensitive is  
 342 FairMIB to variations in hyperparameter settings?

### 343 5.1 EXPERIMENTAL SETTINGS

#### 345 5.1.1 DATASETS AND EVALUATION METRICS

347 We conducted experiments on five widely used benchmark datasets: German Asuncion & Newman  
 348 (2007), Bail Jordan & Freiburger (2015), Credit Yeh & Lien (2009), Pokec-z, and Pokec-n Takac &  
 349 Zabovsky (2012). For model effectiveness, we assess node classification performance using accu-  
 350 racy, F1-score, and AUC-ROC. To evaluate fairness, we adopt Demographic Parity (DP) and Equal  
 351 Opportunity (EO) as metrics (Appendix B), where lower values indicate higher levels of fairness.

#### 353 5.1.2 BASELINES

354 We benchmarked the proposed method against seven state-of-the-art (SOTA) approaches for fair  
 355 node representation learning, including adversarial methods FairGNN Dai & Wang (2021) and  
 356 FairVGNN Wang et al. (2022), data augmentation-based methods NIFTY Agarwal et al. (2021),  
 357 EDITS Dong et al. (2022), and FairGB Li et al. (2024b), an information bottleneck-based method  
 358 GRAFair Zhang et al. (2025), and a disentangled representation learning method DAB-GNN Lee  
 359 et al. (2025).

#### 361 5.1.3 IMPLEMENTATION DETAILS

363 For the German, Bail, Credit, and Pokec datasets, we followed the training, validation, and test set  
 364 splitting scheme proposed in Li et al. (2024b); Yang et al. (2024). For all comparison methods,  
 365 model hyperparameters were either set according to their official implementations or tuned via grid  
 366 search to ensure fairness. All models were optimized using the *Adam* optimizer Kingma & Ba  
 367 (2015), with early stopping based on the validation loss. Following Zhang et al. (2024b), the number  
 368 of hops in the Diffusion View was fixed at  $K = 3$ . To ensure robustness, we report the mean and  
 369 standard deviation over five independent runs with different random seeds. All experiments were  
 370 conducted on an NVIDIA GeForce GTX 4060 GPU (8 GB).

### 371 5.2 RQ1: PERFORMANCE COMPARISON

373 We conducted comprehensive experiments on five benchmark datasets, comparing the proposed  
 374 FairMIB with a standard GCN baseline and seven state-of-the-art fairness-aware methods. The  
 375 results in Table 1 highlight the following key findings: (1) The proposed FairMIB framework  
 376 consistently outperforms the SOTA baselines in terms of fairness while maintaining competitive utility.  
 377 For example, on the German dataset, the proposed method reduces DP and EO by 98.8% and 99.3%  
 378 relative to GCN, and its EO is 75% lower than the best-performing baseline GRAFair. On the

378  
379 Table 1: Comparison of utility and fairness performance across different GNNs fairness methods  
380 on five datasets. The datasets are represented as follows: **I** (German), **II** (Bail), **III** (Credit), **IV**  
381 (Pokec-z), and **V** (Pokec-n). Arrow ( $\uparrow$ ) indicates that higher values are better, while ( $\downarrow$ ) indicates  
382 that lower values are better.

Metrics	Model								
	Vanilla GCN	NIFTY	EDITS	FairGNN	FairGB	GRAFair	DAB-GNN	FairMIB	
<b>I</b>	AUC ( $\uparrow$ ) <b>73.49 <math>\pm</math> 2.15</b>	68.78 $\pm$ 2.69	69.41 $\pm$ 2.33	67.35 $\pm$ 2.13	72.12 $\pm$ 1.10	59.77 $\pm$ 7.59	70.32 $\pm$ 1.12	66.59 $\pm$ 4.30	65.55 $\pm$ 1.61
	F1 ( $\uparrow$ ) 80.76 $\pm$ 2.35	81.40 $\pm$ 0.50	81.55 $\pm$ 0.59	82.01 $\pm$ 0.26	82.14 $\pm$ 0.42	<b>82.46 <math>\pm</math> 0.23</b>	81.95 $\pm$ 0.33	82.16 $\pm$ 0.33	82.45 $\pm$ 0.20
	ACC ( $\uparrow$ ) <b>71.04 <math>\pm</math> 2.36</b>	69.92 $\pm$ 1.14	70.22 $\pm$ 0.89	69.68 $\pm$ 0.30	70.16 $\pm$ 0.86	70.01 $\pm$ 0.73	70.06 $\pm$ 0.16	70.12 $\pm$ 0.63	70.24 $\pm$ 0.48
	DP ( $\downarrow$ ) 33.75 $\pm$ 12.34	5.73 $\pm$ 5.25	4.05 $\pm$ 4.48	3.49 $\pm$ 2.15	1.68 $\pm$ 0.98	1.68 $\pm$ 3.30	0.91 $\pm$ 0.47	1.19 $\pm$ 1.25	<b>0.38 <math>\pm</math> 0.76</b>
	EO ( $\downarrow$ ) 25.73 $\pm$ 8.36	5.08 $\pm$ 4.29	3.89 $\pm$ 4.23	3.40 $\pm$ 2.15	1.21 $\pm$ 2.11	1.08 $\pm$ 1.80	<b>0.68 <math>\pm</math> 0.56</b>	1.18 $\pm$ 1.75	<b>0.17 <math>\pm</math> 0.34</b>
<b>II</b>	AUC ( $\uparrow$ ) 87.39 $\pm$ 0.17	78.20 $\pm$ 2.78	86.44 $\pm$ 2.17	87.36 $\pm$ 0.90	85.68 $\pm$ 0.37	87.68 $\pm$ 1.41	88.68 $\pm$ 1.35	89.08 $\pm$ 3.34	<b>89.18 <math>\pm</math> 2.15</b>
	F1 ( $\uparrow$ ) 77.63 $\pm$ 0.42	64.76 $\pm$ 3.91	75.58 $\pm$ 3.77	77.50 $\pm$ 1.69	79.11 $\pm$ 0.33	77.08 $\pm$ 2.00	80.03 $\pm$ 0.56	79.79 $\pm$ 2.02	<b>80.10 <math>\pm</math> 1.25</b>
	ACC ( $\uparrow$ ) 82.58 $\pm$ 1.21	74.19 $\pm$ 2.57	84.49 $\pm$ 2.27	82.94 $\pm$ 1.67	84.73 $\pm$ 0.46	83.31 $\pm$ 1.90	83.97 $\pm$ 1.90	<b>89.73 <math>\pm</math> 1.02</b>	<b>85.62 <math>\pm</math> 0.81</b>
	DP ( $\downarrow$ ) 6.94 $\pm$ 0.21	2.44 $\pm$ 1.29	6.64 $\pm$ 0.39	6.90 $\pm$ 0.17	6.53 $\pm$ 0.67	5.17 $\pm$ 0.36	1.32 $\pm$ 0.43	<b>0.92 <math>\pm</math> 0.53</b>	<b>1.23 <math>\pm</math> 0.49</b>
	EO ( $\downarrow$ ) 5.56 $\pm$ 0.37	1.72 $\pm$ 1.08	7.51 $\pm$ 1.20	4.65 $\pm$ 0.14	4.95 $\pm$ 1.22	3.44 $\pm$ 1.20	1.46 $\pm$ 0.28	<b>1.26 <math>\pm</math> 0.38</b>	<b>1.17 <math>\pm</math> 0.45</b>
<b>III</b>	AUC ( $\uparrow$ ) 72.80 $\pm$ 0.23	71.96 $\pm$ 0.19	73.01 $\pm$ 0.11	71.95 $\pm$ 1.43	71.34 $\pm$ 0.41	<b>73.21 <math>\pm</math> 0.83</b>	72.04 $\pm$ 0.42	71.34 $\pm$ 0.76	<b>73.49 <math>\pm</math> 0.51</b>
	F1 ( $\uparrow$ ) 82.93 $\pm$ 0.21	81.72 $\pm$ 0.05	81.81 $\pm$ 0.28	81.84 $\pm$ 1.19	87.08 $\pm$ 0.74	85.83 $\pm$ 3.34	<b>87.44 <math>\pm</math> 0.23</b>	87.28 $\pm$ 1.06	<b>87.79 <math>\pm</math> 0.27</b>
	ACC ( $\uparrow$ ) 73.99 $\pm$ 0.01	73.45 $\pm$ 0.06	73.51 $\pm$ 0.30	73.41 $\pm$ 1.24	78.04 $\pm$ 0.33	77.54 $\pm$ 3.48	77.34 $\pm$ 1.43	<b>78.28 <math>\pm</math> 1.37</b>	<b>78.57 <math>\pm</math> 0.86</b>
	DP ( $\downarrow$ ) 12.53 $\pm$ 0.25	11.68 $\pm$ 0.07	10.90 $\pm$ 1.22	12.64 $\pm$ 2.11	5.02 $\pm$ 5.22	2.30 $\pm$ 3.00	1.06 $\pm$ 0.71	<b>0.67 <math>\pm</math> 0.76</b>	<b>0.40 <math>\pm</math> 0.69</b>
	EO ( $\downarrow$ ) 10.63 $\pm$ 0.02	9.39 $\pm$ 0.07	8.75 $\pm$ 1.21	10.41 $\pm$ 2.03	3.60 $\pm$ 4.31	1.75 $\pm$ 2.07	0.64 $\pm$ 0.26	<b>0.49 <math>\pm</math> 0.68</b>	<b>0.24 <math>\pm</math> 0.48</b>
<b>IV</b>	AUC ( $\uparrow$ ) 72.42 $\pm$ 0.33	71.59 $\pm$ 0.17	OOM	73.12 $\pm$ 0.12	<b>76.02 <math>\pm</math> 0.16</b>	OOM	69.11 $\pm$ 2.27	72.02 $\pm$ 0.22	73.15 $\pm$ 1.64
	F1 ( $\uparrow$ ) 70.32 $\pm$ 0.20	67.13 $\pm$ 1.66	OOM	67.65 $\pm$ 1.65	<b>70.45 <math>\pm</math> 0.57</b>	OOM	64.21 $\pm$ 1.53	64.57 $\pm$ 1.76	68.86 $\pm$ 1.40
	ACC ( $\uparrow$ ) <b>68.54 <math>\pm</math> 0.32</b>	66.24 $\pm$ 0.34	OOM	66.24 $\pm$ 0.34	<b>68.24 <math>\pm</math> 0.17</b>	OOM	62.29 $\pm$ 0.17	67.34 $\pm$ 1.33	66.16 $\pm$ 1.43
	DP ( $\downarrow$ ) 4.21 $\pm$ 0.32	6.50 $\pm$ 2.16	OOM	2.73 $\pm$ 2.23	2.90 $\pm$ 0.77	OOM	<b>1.41 <math>\pm</math> 1.73</b>	1.55 $\pm$ 0.45	<b>0.69 <math>\pm</math> 0.26</b>
	EO ( $\downarrow$ ) 4.29 $\pm$ 0.24	6.43 $\pm$ 1.73	OOM	2.17 $\pm$ 1.85	3.09 $\pm$ 0.97	OOM	1.73 $\pm$ 1.49	<b>1.12 <math>\pm</math> 0.77</b>	<b>0.52 <math>\pm</math> 0.38</b>
<b>V</b>	AUC ( $\uparrow$ ) 72.12 $\pm$ 0.57	71.28 $\pm$ 0.35	OOM	71.49 $\pm$ 0.28	<b>73.22 <math>\pm</math> 0.92</b>	OOM	72.28 $\pm$ 1.46	73.11 $\pm$ 0.36	<b>73.28 <math>\pm</math> 1.02</b>
	F1 ( $\uparrow$ ) 66.78 $\pm$ 1.09	64.02 $\pm$ 1.26	OOM	64.80 $\pm$ 0.89	<b>63.35 <math>\pm</math> 1.64</b>	OOM	65.75 $\pm$ 1.71	<b>68.62 <math>\pm</math> 1.22</b>	<b>69.02 <math>\pm</math> 1.91</b>
	ACC ( $\uparrow$ ) 66.22 $\pm$ 1.09	66.14 $\pm$ 0.49	OOM	65.36 $\pm$ 2.06	66.16 $\pm$ 0.72	OOM	66.21 $\pm$ 2.35	<b>67.23 <math>\pm</math> 0.81</b>	66.37 $\pm$ 1.09
	DP ( $\downarrow$ ) 2.83 $\pm$ 0.46	1.62 $\pm$ 0.94	OOM	2.26 $\pm$ 1.19	4.28 $\pm$ 1.33	OOM	3.22 $\pm$ 1.18	1.57 $\pm$ 0.73	<b>1.12 <math>\pm</math> 0.76</b>
	EO ( $\downarrow$ ) 3.66 $\pm$ 0.43	1.83 $\pm$ 1.12	OOM	3.21 $\pm$ 2.28	5.34 $\pm$ 1.27	OOM	2.65 $\pm$ 1.07	1.36 $\pm$ 0.54	0.92 $\pm$ 0.90

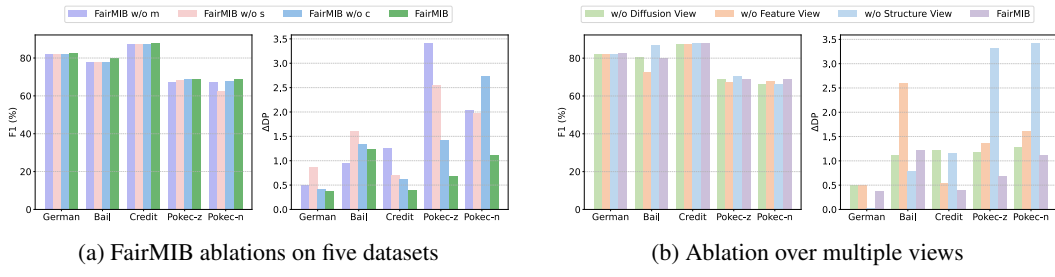


Figure 2: Ablation study and multi-view study on FairMIB

Bail dataset, FairMIB achieves an EO reduction of 82.3% over GCN, while improving F1-score by 3.2%, surpassing all other fairness-aware methods. (2) The proposed FairMIB framework demonstrates strong scalability and utility preservation on large-scale datasets. For instance, on the Pokec-n dataset, it improves the F1-score by 3.4% over GCN and achieves the best fairness, with an EO value 32.4% lower than the runner-up model, DAB-GNN. Similarly, on the Pokec-z dataset, its DP and EO metrics are 51.1% and 53.6% lower than the strongest competitors, respectively. These results confirm the superior balance and scalability of our approach on large-scale graphs.

### 5.3 RQ2: ABLATION STUDY

To answer RQ2, we conducted ablations on our FairMIB with three variants: FairMIB w/o m (removing information compression), FairMIB w/o s (removing the conditional constraint), and FairMIB w/o c (removing Multi-view consistency). As shown in Figure 2a, removing the conditional module (w/o s) significantly degrades fairness across datasets; for example, DP worsens by over 30% on Bail, confirming the need to maximize  $I(\mathbf{Y}; \mathbf{Z} | \mathbf{S})$  by conditioning on  $\mathbf{S}$ . Removing compression (w/o m), which minimizes  $I(\{\mathcal{G}_{\text{View}}\}; \mathbf{Z})$ , harms both utility and fairness, most notably on Pokec-z where DP nearly quadruples, showing that filtering redundant information improves both. Removing consistency (w/o c) also reduces fairness, especially on Pokec-n where DP and EO are worse than other variants, indicating that contrastive alignment of view specific representations yields a robust shared latent space. Overall, these studies verify that the conditional bottleneck, compression, and Multi-view consistency work together to mitigate sensitive attribute bias by enforcing the fairness objective, filtering irrelevant information, and aligning Multi-view semantics.

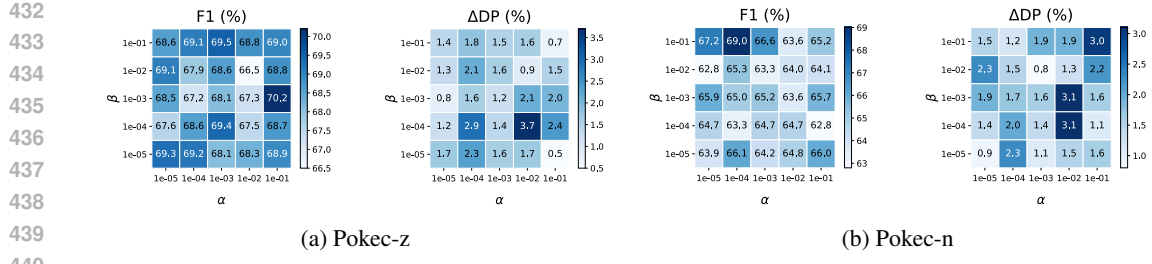


Figure 3: Parameter sensitivity results on Pokec datasets. Results demonstrate that FairMIB achieves stable performance across a wide range of parameter settings.

#### 5.4 RQ3: MULTI-VIEW ANALYSIS

To answer RQ3, we conducted ablation experiments by removing the Diffusion View (w/o Diffusion View), Feature View (w/o Feature View), or Structural View (w/o Structure View). The results in Figure 2b show that the three views provide complementary information, and their combination is essential for balancing utility and fairness. Removing any view typically leads to a significant performance drop. For example, on the Bail dataset, removing the Feature View causes a 10% drop in F1-score and deterioration in DP and EO metrics, indicating the importance of node attributes for fair decision-making. The relative importance of the Structural and Diffusion Views varies across datasets. On the Pokec-z and Pokec-n datasets, removing the Structural View worsens DP by over 380% and 205%, respectively, showing that structural bias is critical in these topologies. In contrast, on the Credit dataset, removing the Diffusion View has the largest negative impact on fairness, increasing DP by 205%, highlighting the role of multi-hop information propagation in bias correction. These results demonstrate that no single view is universally dominant, validating the necessity of our Multi-view decoupling framework.

#### 5.5 RQ4: HYPER-PARAMETER SENSITIVITY ANALYSIS

To address RQ4, we perform a sensitivity analysis of FairMIB with respect to two key hyperparameters,  $\alpha$  and  $\beta$ , which control the relative contributions of information compression and view alignment, respectively. Specifically, we evaluate the model by varying  $\alpha$  and  $\beta$  across the set  $10^{-1}, 10^{-2}, 10^{-3}, 10^{-4}, 10^{-5}$  on the Bail, Credit, Pokec-z, and Pokec-n datasets. The results, shown in Figure 3, indicate that FairMIB exhibits robust performance across a wide range of these hyperparameter values. However, setting  $\alpha$  and  $\beta$  excessively high can lead to performance degradation due to over-compression of information and overly strict enforcement of view alignment. These findings underscore the importance of balancing the two components, suggesting that selecting  $\alpha$  and  $\beta$  within the range of  $10^{-3}$  to  $10^{-5}$  achieves a trade-off between utility and fairness.

#### 5.6 EFFICIENCY ANALYSIS

In terms of time and space complexity, the main computational cost of FairMIB comes from the APPNP-based feature diffusion and the forward and backward passes of the three encoders. For each training epoch, applying  $K$ -step APPNP on the weighted features over the graph  $\mathcal{G} = (\mathcal{V}, \mathcal{E}, \mathbf{X})$  has a computational complexity of approximately  $\mathcal{O}(K(m + n)h)$ , where  $n = |\mathcal{V}|$  is the number of nodes,  $m = |\mathcal{E}|$  is the number of edges, and  $h$  denotes the hidden dimension. The three encoders process the raw features  $\mathbf{X}$ , the diffused features, and the all-one features, respectively. Their computational cost grows linearly with the number of nodes and edges, approximately  $\mathcal{O}(ndh + mh)$ . Adding the computation for the contrastive loss, the KL regularization, and the classifier, which together require  $\mathcal{O}(nh)$ , the overall complexity remains nearly linear with respect to graph size. When considering  $R$  independent runs and  $T$  training epochs, the total time complexity of FairMIB becomes  $\mathcal{O}(RT(Kmh + ndh))$ . The memory complexity is  $\mathcal{O}(n(d + 3h) + m)$ , which is on the same order as standard multi-branch GNNs. The propensity score model is pre-trained separately for about 100 steps before the main training process, and this one-time cost is negligible compared with the full training procedure. As shown in Figure 4, we compare the actual running times of different fair graph learning methods under the same settings. The results demonstrate that, while

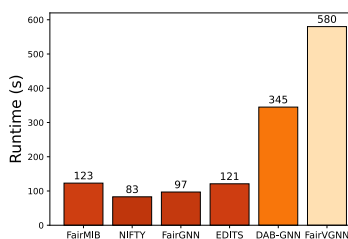


Figure 4: Comparison of Time costs for FairMIB and baselines on Bail

achieving Multi-view representation learning, FairMIB maintains linear scalability comparable to standard graph neural networks and is more efficient than several more complex fair GNN models.

### 5.7 WHY CHOOSE APPNP

We adopt APPNP to model higher-order neighborhood effects in a stable and efficient way. We conduct an ablation study on the Bail dataset with five propagation operators: GCN, APPNP, without IPW, SGC, and GCNII in Table 2. APPNP provides the best trade-off among utility, fairness, and efficiency. Compared with GCN, APPNP increases AUC by about 1% and F1 by roughly 1.5%, while reducing training time by over 5% and slightly lowering both fairness gaps (around 10–15% smaller DP and about 7% smaller EO). SGC is roughly 7% faster than APPNP, but suffers from about 2% lower AUC and more than 25% DP gap, indicating that overly aggressive simplification harms fair representation learning. GCNII offers less than 1% additional AUC over APPNP but requires approximately 17% more training time and a considerably more complex architecture. To isolate the effect of the IPW module, we compare APPNP with and without IPW. Introducing IPW reduces the demographic parity gap by nearly 30% and the equal opportunity gap by about 20%, showing that IPW effectively mitigates bias accumulated during diffusion. Overall, APPNP with IPW forms a principled compromise that balances accuracy, fairness, and efficiency while remaining modular.

Table 2: Ablation study for choosing APPNP

Metric	APPNP	GCN	SGC	GCNII	Without IPW
AUC	$88.52 \pm 1.45$	$87.60 \pm 2.11$	$86.88 \pm 1.92$	$89.09 \pm 2.09$	$88.26 \pm 0.93$
ACC	$84.48 \pm 1.53$	$83.50 \pm 2.43$	$84.03 \pm 1.47$	$85.49 \pm 3.15$	$84.54 \pm 1.46$
F1	$78.89 \pm 1.91$	$77.62 \pm 3.11$	$76.61 \pm 2.27$	$80.27 \pm 3.69$	$78.91 \pm 1.36$
DP	$1.35 \pm 1.23$	$1.53 \pm 0.84$	$1.72 \pm 1.45$	$1.31 \pm 0.35$	$1.90 \pm 0.75$
EO	$1.39 \pm 0.68$	$1.49 \pm 0.66$	$2.86 \pm 2.01$	$1.39 \pm 0.49$	$1.72 \pm 0.74$
Time (s)	123.4915	130.2052	115.1629	144.9692	120.7191

## 6 CONCLUSION

This paper addresses the challenge of bias in GNNs from a fairness perspective originating from multi-source information. Traditional approaches often fail to disentangle distinct sources of bias, leading to a suboptimal trade-off between model utility and fairness. To overcome this, we propose FairMIB, a novel framework grounded in the Multi-view conditional information bottleneck principle. Our FairMIB method first disentangles composite graph data into independent feature, structural, and Diffusion Views. It then applies a conditional information bottleneck to the fusion representation to learn compressed representations that preserve task-relevant information while mitigating sensitive attribute leakage. Furthermore, we introduce a Multi-view consistency constraint to ensure semantic alignment across the learned representations. Extensive experiments on five benchmark datasets demonstrate that FairMIB consistently outperforms state-of-the-art methods, achieving a superior balance between fairness and utility. While these results are promising, several avenues for future work remain. The current framework could be extended to more complex scenarios involving multiple intersecting sensitive attributes or enhanced by exploring more diverse strategies for view generation.

540 7 ETHICS STATEMENT  
541542 This work investigates fair learning on graphs and proposes a Multi-view conditional information  
543 bottleneck for mitigating bias. We use only publicly available datasets under their licenses and do  
544 not collect new human subject data. Sensitive attributes are used only during training to encourage  
545 conditional fairness and are not required at inference time. We evaluate demographic parity and  
546 equality of opportunity, but fairness is context dependent and our results do not guarantee fairness in  
547 all deployments. Practitioners should verify consent and data provenance, apply privacy safeguards,  
548 conduct domain-specific audits with affected stakeholders, and avoid presenting improvements on  
549 chosen metrics as proof of overall neutrality.  
550551 8 REPRODUCIBILITY STATEMENT  
552553 We describe all model components, objectives, and training protocols, including architectures,  
554 losses, data preprocessing, and evaluation metrics. We will release code, configuration files, and  
555 experiment scripts that reproduce main tables, ablations, and sensitivity analyses with fixed random  
556 seeds, reported means and standard deviations over multiple runs, and the exact data splits used. The  
557 repository will include a dependency file with package versions, instructions for environment setup,  
558 and commands for end-to-end execution on commodity GPUs, enabling independent verification  
559 and extension of our results. Our implementation has been submitted in OpenReview and the code  
560 will be made publicly available on GitHub.  
561

## 562 REFERENCES

563 Chirag Agarwal, Himabindu Lakkaraju, and Marinka Zitnik. Towards a unified framework for fair  
564 and stable graph representation learning. In *Uncertainty in artificial intelligence*, pp. 2114–2124.  
565 PMLR, 2021.  
566  
567 Amina Amara, Mohamed Ali Hadj Taieb, and Mohamed Ben Aouicha. A multi-view gnn-based  
568 network representation learning framework for recommendation systems. *Neurocomputing*, 619:  
569 129001, 2025.  
570  
571 Arthur Asuncion and David Newman. Uci machine learning repository, 2007.  
572  
573 Kamalika Chaudhuri, Sham M Kakade, Karen Livescu, and Karthik Sridharan. Multi-view cluster-  
574 ing via canonical correlation analysis. In *Proceedings of the 26th annual international conference*  
575 *on machine learning*, pp. 129–136, 2009.  
576  
577 Qingfeng Chen, Shiyuan Li, Yixin Liu, Shirui Pan, Geoffrey I Webb, and Shichao Zhang.  
578 Uncertainty-aware graph neural networks: A multihop evidence fusion approach. *IEEE Transac-  
579 tions on Neural Networks and Learning Systems*, 2025.  
580  
581 Chenzhang Cui, Yazhou Ren, Jingyu Pu, Jiawei Li, Xiaorong Pu, Tianyi Wu, Yutao Shi, and Lifang  
582 He. A novel approach for effective multi-view clustering with information-theoretic perspec-  
583 tive. In *Advances in Neural Information Processing Systems 36: Annual Conference on Neural*  
584 *Information Processing Systems, NeurIPS, New Orleans, LA, USA, December 10 - 16*, 2023.  
585  
586 Enyan Dai and Suhang Wang. Say no to the discrimination: Learning fair graph neural networks with  
587 limited sensitive attribute information. In *Proceedings of the 14th ACM international conference*  
588 *on web search and data mining*, pp. 680–688, 2021.  
589  
590 Yushun Dong, Ninghao Liu, Brian Jalaian, and Jundong Li. Edits: Modeling and mitigating data  
591 bias for graph neural networks. In *Proceedings of the ACM web conference*, pp. 1259–1269, 2022.  
592  
593 Cynthia Dwork, Moritz Hardt, Toniann Pitassi, et al. Fairness through awareness. In *Proceedings*  
594 *of the 3rd innovations in theoretical computer science conference*, pp. 214–226, 2012.  
595  
596 Marco Federici, Anjan Dutta, Patrick Forré, Nate Kushman, and Zeynep Akata. Learning robust rep-  
597 resentations via multi-view information bottleneck. In *8th International Conference on Learning*  
598 *Representations, ICLR, Addis Ababa, Ethiopia, April 26-30*. OpenReview.net, 2020.

594 Yan Feng and Quan Qian. Ppfedggn: An efficient privacy-preserving federated graph neural network  
 595 method for social network analysis. *IEEE Transactions on Computational Social Systems*, 2025.  
 596

597 Borja Rodríguez Gálvez, Ragnar Thobaben, and Mikael Skoglund. A variational approach to privacy  
 598 and fairness. In *IEEE Information Theory Workshop, ITW, Kanazawa, Japan, October 17-21*, pp.  
 599 1–6, 2021.

600 Zhimeng Guo, Jialiang Li, Teng Xiao, Yao Ma, and Suhang Wang. Towards fair graph neural  
 601 networks via graph counterfactual. In *Proceedings of the 32nd ACM international conference on*  
 602 *information and knowledge management*, pp. 669–678, 2023.  
 603

604 Moritz Hardt, Eric Price, and Nati Srebro. Equality of opportunity in supervised learning. In  
 605 Daniel D. Lee, Masashi Sugiyama, Ulrike von Luxburg, Isabelle Guyon, and Roman Garnett  
 606 (eds.), *Advances in Neural Information Processing Systems 29: Annual Conference on Neural*  
 607 *Information Processing Systems, December 5-10, Barcelona, Spain*, pp. 3315–3323, 2016.

608 Zhimeng Jiang, Xiaotian Han, Chao Fan, Zirui Liu, Na Zou, Ali Mostafavi, and Xia Hu. Chasing  
 609 fairness in graphs: A gnn architecture perspective. In *Proceedings of the AAAI Conference on*  
 610 *Artificial Intelligence*, volume 38, pp. 21214–21222, 2024.  
 611

612 Kareem L Jordan and Tina L Freiburger. The effect of race/ethnicity on sentencing: Examining  
 613 sentence type, jail length, and prison length. *Journal of Ethnicity in Criminal Justice*, (3):179–  
 614 196, 2015.

615 Wei Ju, Yifan Wang, Yifang Qin, Zhengyang Mao, Zhiping Xiao, Junyu Luo, Junwei Yang, Yiyang  
 616 Gu, Dongjie Wang, Qingqing Long, Siyu Yi, Xiao Luo, and Ming Zhang. Towards graph con-  
 617 trastive learning: A survey and beyond. *CoRR*, abs/2405.11868, 2024a.  
 618

619 Wei Ju, Siyu Yi, Yifan Wang, Zhiping Xiao, Zhengyang Mao, Hourun Li, Yiyang Gu, Yifang Qin,  
 620 Nan Yin, Senzhang Wang, et al. A survey of graph neural networks in real world: Imbalance,  
 621 noise, privacy and ood challenges. *arXiv preprint arXiv:2403.04468*, 2024b.

622 Kenji Kawaguchi, Zhun Deng, Xu Ji, and Jiaoyang Huang. How does information bottleneck help  
 623 deep learning? In *International conference on machine learning*, pp. 16049–16096. PMLR, 2023.  
 624

625 Diederik P. Kingma and Jimmy Ba. Adam: A method for stochastic optimization. In *3rd Interna-  
 626 tional Conference on Learning Representations, ICLR, San Diego, CA, USA, May 7-9, Conference*  
 627 *Track Proceedings*, 2015.

628 Thomas N. Kipf and Max Welling. Variational graph auto-encoders. *CoRR*, 2016.  
 629

630 Johannes Klicpera, Aleksandar Bojchevski, and Stephan Günnemann. Predict then propagate:  
 631 Graph neural networks meet personalized pagerank. In *7th International Conference on Learning*  
 632 *Representations, ICLR, New Orleans, LA, USA, May 6-9*. OpenReview.net, 2019.  
 633

634 Yeon-Chang Lee, Hojung Shin, and Sang-Wook Kim. Disentangling, amplifying, and debiasing:  
 635 Learning disentangled representations for fair graph neural networks. In *Proceedings of the AAAI*  
 636 *Conference on Artificial Intelligence*, volume 39, pp. 12013–12021, 2025.

637 Chunxiao Li, Hongchang Wang, Songtao Jiang, and Bin Gu. The effect of ai-enabled credit scor-  
 638 ing on financial inclusion: Evidence from an underserved population of over one million. *MIS*  
 639 *Quarterly*, 48(4):1803–1834, 2024a.

640 Fan Li, Kari Lock Morgan, and Alan M Zaslavsky. Balancing covariates via propensity score weight-  
 641 ing. *Journal of the American Statistical Association*, 113(521):390–400, 2018.  
 642

643 Zhixun Li, Yushun Dong, Qiang Liu, and Jeffrey Xu Yu. Rethinking fair graph neural networks from  
 644 re-balancing. In *Proceedings of the 30th ACM SIGKDD Conference on Knowledge Discovery and*  
 645 *Data Mining*, pp. 1736–1745, 2024b.

646 Richard F Lowden. Risk assessment algorithms: The answer to an inequitable bail system? *North*  
 647 *Carolina Journal of Law & Technology*, 19(4):221, 2018.

648 Yujie Mo, Heng Tao Shen, and Xiaofeng Zhu. Efficient self-supervised heterogeneous graph repre-  
 649 sentation learning with reconstruction. *Information Fusion*, 117:102846, 2025.  
 650

651 Tahleen A. Rahman, Bartłomiej Surma, Michael Backes, and Yang Zhang. Fairwalk: Towards fair  
 652 graph embedding. In Sarit Kraus (ed.), *Proceedings of the Twenty-Eighth International Joint  
 653 Conference on Artificial Intelligence, IJCAI, Macao, China, August 10-16*, pp. 3289–3295, 2019.

654 Evgenia Rusak, Patrik Reizinger, Attila Juhos, Oliver Bringmann, Roland S. Zimmermann, and  
 655 Wieland Brendel. Infonce: Identifying the gap between theory and practice. In *International  
 656 Conference on Artificial Intelligence and Statistics, AISTATS, Mai Khao, Thailand, 3-5 May*,  
 657 volume 258 of *Proceedings of Machine Learning Research*, pp. 4159–4167. PMLR, 2025.  
 658

659 Lubos Takac and Michal Zabovsky. Data analysis in public social networks. In *International sci-  
 660 entific conference and international workshop present day trends of innovations*, number 6, 2012.

661 Conghao Wang, Gaurav Asok Kumar, and Jagath C Rajapakse. Drug discovery and mechanism  
 662 prediction with explainable graph neural networks. *Scientific Reports*, 15(1):179, 2025.  
 663

664 Yu Wang, Yuying Zhao, Yushun Dong, Huiyuan Chen, Jundong Li, and Tyler Derr. Improving  
 665 fairness in graph neural networks via mitigating sensitive attribute leakage. In *Proceedings of the  
 666 28th ACM SIGKDD conference on knowledge discovery and data mining*, pp. 1938–1948, 2022.

667 Zichong Wang, Zhipeng Yin, Yuying Zhang, Liping Yang, Tingting Zhang, Niki Pissinou, Yu Cai,  
 668 Shu Hu, Yun Li, Liang Zhao, and Wenbin Zhang. Fg-smote: Towards fair node classification with  
 669 graph neural network. *SIGKDD Explor.*, 26(2):99–108, 2024.

670 Tailin Wu, Hongyu Ren, Pan Li, and Jure Leskovec. Graph information bottleneck. *Advances in  
 671 Neural Information Processing Systems*, 33:20437–20448, 2020a.  
 672

673 Zonghan Wu, Shirui Pan, Fengwen Chen, Guodong Long, Chengqi Zhang, and Philip S Yu. A  
 674 comprehensive survey on graph neural networks. *IEEE transactions on neural networks and  
 675 learning systems*, 32(1):4–24, 2020b.

676 Junsong Xie, Yonghui Yang, Zihan Wang, and Le Wu. Learning fair representations for recom-  
 677 mendation via information bottleneck principle. In *Proceedings of the Thirty-Third International  
 678 Joint Conference on Artificial Intelligence*, pp. 2469–2477, 2024.  
 679

680 Cheng Yang, Jixi Liu, Yunhe Yan, and Chuan Shi. Fairsin: Achieving fairness in graph neural  
 681 networks through sensitive information neutralization. In *Proceedings of the AAAI Conference on  
 682 Artificial Intelligence*, pp. 9241–9249, 2024.

683 I-Cheng Yeh and Che-hui Lien. The comparisons of data mining techniques for the predictive  
 684 accuracy of probability of default of credit card clients. *Expert systems with applications*, (2):  
 685 2473–2480, 2009.  
 686

687 Mengmeng Zhan, Zongqian Wu, Jiaying Yang, Lin Peng, Jialie Shen, and Xiaofeng Zhu. Dual  
 688 transferable knowledge interaction for source-free domain adaptation. *Information Processing &  
 689 Management*, 63(1):104302, 2026.

690 Guixian Zhang, Debo Cheng, Guan Yuan, and Shichao Zhang. Learning fair representations via  
 691 rebalancing graph structure. *Information Processing & Management*, 61(1):103570, 2024a.  
 692

693 Guixian Zhang, Guan Yuan, Debo Cheng, Ludan He, Rui Bing, Jiuyong Li, and Shichao Zhang.  
 694 Multi-view graph neural network for fair representation learning. In *Asia-Pacific Web (APWeb)  
 695 and Web-Age Information Management (WAIM) Joint International Conference on Web and Big  
 696 Data*, pp. 208–223. Springer, 2024b.

697 He Zhang, Bang Wu, Xingliang Yuan, Shirui Pan, Hanghang Tong, and Jian Pei. Trustworthy graph  
 698 neural networks: Aspects, methods, and trends. *Proceedings of the IEEE*, 112(2):97–139, 2024c.  
 699

700 Ziyi Zhang, Mingxuan Ouyang, Wanyu Lin, Hao Lan, and Lei Yang. Debiasing graph representation  
 701 learning based on information bottleneck. *IEEE transactions on neural networks and learning  
 systems*, 36(6):11092–11105, 2025.

702 Ying Zhen, Yuchang Zhu, Jintang Li, and Liang Chen. Fairdla: Improving the fairness-utility trade-  
 703 off in graph neural networks via dual-level alignment. *Knowledge-Based Systems*, pp. 113768,  
 704 2025.

705 Lijing Zheng, Jihong Wang, Huan Liu, and Minnan Luo. Disentangled counterfactual graph aug-  
 706mentation framework for fair graph learning with information bottleneck. In *Joint European Con-  
 707ference on Machine Learning and Knowledge Discovery in Databases*, pp. 387–405. Springer,  
 708 2024.

709 Jie Zhou, Ganqu Cui, Shengding Hu, Zhengyan Zhang, Cheng Yang, Zhiyuan Liu, Lifeng Wang,  
 710 Changcheng Li, and Maosong Sun. Graph neural networks: A review of methods and applica-  
 711tions. *AI open*, 1:57–81, 2020.

712 Yuchang Zhu, Jintang Li, Zibin Zheng, and Liang Chen. Fair graph representation learning via  
 713 sensitive attribute disentanglement. In *Proceedings of the ACM Web Conference*, pp. 1182–1192,  
 714 2024.

715

716

717

718

719

## 720 Appendix

721

722 This is the appendix to the paper ‘Learning Fair Graph Representations with Multi-  
 723 view Information Bottleneck’. This appendix provides additional details on related  
 724 work, preliminaries, the proposed method, and extended experimental results.

725

726

## 727 A RELATED WORK

728

### 729 A.1 FAIRNESS IN GNNS

730

731 In recent years, research on fairness in GNNs has accelerated, with methods com-  
 732 monly grouped into two categories: pre-processing Li et al. (2024b); Dong et al.  
 733 (2022) and in-processing Yang et al. (2024); Agarwal et al. (2021); Wang et al.  
 734 (2022). Pre-processing methods address fairness at the data level by rebalancing  
 735 attribute distributions or modifying graph structures before model training. These  
 736 methods aim to reduce the unfairness induced by distributional disparities and struc-  
 737 tural homophily. For example, EDITS Dong et al. (2022) introduces a debiasing  
 738 framework that jointly optimizes attribute reweighting and structural perturbation in  
 739 order to reduce attribute and structural bias in graph data. More recently, FairGB Li  
 740 et al. (2024b) approaches the problem from the perspective of data generation and  
 741 sampling by combining resampling with causally inspired contrastive generation.  
 742 This method not only alleviates group bias caused by imbalance in the training  
 743 set but also provides a more neutral training view for subsequent model learning. A  
 744 common characteristic of these approaches is the direct modification of input distri-  
 745 butions or graph connectivity patterns, thereby ensuring that any downstream GNN  
 746 can be trained on a relatively fair dataset.

747

748

749

750

751 In-processing methods, in contrast, introduce fairness constraints or architectural  
 752 designs during model learning to suppress the leakage of sensitive information in  
 753 the message-passing stage Wang et al. (2022); Agarwal et al. (2021); Yang et al.  
 754 (2024); Zhu et al. (2024); Lee et al. (2025). Since feature propagation can trans-  
 755 form channels originally uncorrelated with sensitive attributes into biased ones,

many approaches aim to limit the reliance of propagation channels on sensitive cues. For example, FairVGNN Wang et al. (2022) leverages correlations before and after propagation to learn channel masks that reduce the dependence on sensitive features. NIFTY Agarwal et al. (2021) employs adversarial and counterfactual augmentations to stabilize embeddings and mitigate group separability. FairSIN Yang et al. (2024) proposes a neutralization paradigm that constructs and injects fairness-promoting features from heterogeneous neighbors prior to message passing, thereby offsetting sensitive bias signals and supplementing non-sensitive information.

More recently, disentanglement-based approaches have gained attention. FairSAD Zhu et al. (2024) disentangles sensitive-related information into independent components in the representation space and applies channel-wise masking to de-correlate them, thus enhancing fairness while preserving task-relevant signals. DAB-GNN Lee et al. (2025) further disentangles attribute bias, structural bias, and their interactions, explicitly amplifies these components, and then performs distribution alignment and contrastive regularization for debiasing, achieving fine-grained fairness control in an end-to-end manner.

Overall, pre-processing methods mitigate unfairness at the data level by modifying distributions or structures before training, while in-processing methods act directly within the learning process through fairness-aware regularization, loss constraints, or architectural redesigns. Together, these strategies highlight complementary perspectives on mitigating bias in GNNs.

## A.2 FAIRNESS IN INFORMATION BOTTLENECK

The fundamental principle of the IB framework is to identify a minimal sufficient representation that optimizes the compression of input data while preserving only the most critical information necessary for subsequent tasks Kawaguchi et al. (2023). The application of this principle to graph-structured data poses unique challenges, as the non-independent and identically distributed (NIID) nature of graphs complicates traditional optimization methods Xie et al. (2024). In order to address this issue, researchers have proposed the Graph Information Bottleneck (GIB) model Wu et al. (2020a), which extends IB to graph learning by simultaneously compressing node features and structural information.

In the pursuit of fair graph representation learning, IB theory demonstrates considerable potential due to its capacity to accurately quantify and regulate the information contained within a representation, thereby facilitating a more optimal balance between model utility and fairness Jiang et al. (2024). In order to achieve this objective in a stable manner, frameworks such as GRAFair Zhang et al. (2025) employ a variational graph autoencoder architecture. This architecture renders the optimization process tractable and effectively circumvents the instability issues that are prevalent in adversarial learning. Recent research has combined the IB principle with disentanglement learning and counterfactual augmentation to enhance the debiasing process. For instance, FDGIB Zheng et al. (2024) employs IB theory to direct the model in decomposing node representations into two distinct subspaces: one correlated with the sensitive attribute and one independent of it. Despite these

advances, single-view or single-embedding processing remains limited in its capacity. Graph bias is multi-source, and reliance on a single desensitized representation can lead to the conflation of signals from different origins, resulting in under-correction and residual leakage.

## B PRELIMINARIES

### B.1 FAIRNESS METRICS

To evaluate the fairness of our model, we focus on Group Fairness, which aims to ensure that the model’s predictions are not biased against any specific group. In the node classification task, we adopt two widely used fairness metrics: Demographic Parity Dwork et al. (2012) and Equal Opportunity Hardt et al. (2016).

Here, we consider a common binary classification scenario where  $s \in \{0, 1\}$  represents the sensitive attribute of a node (e.g., two different demographic groups),  $y \in \{0, 1\}$  denotes the ground-truth label, and  $\hat{y} \in \{0, 1\}$  is the predicted label given by the model.

#### B.1.1 DEMOGRAPHIC PARITY (DP)

The core idea of Demographic Parity is that the model prediction  $\hat{y}$ , should be statistically independent of the sensitive attribute  $s$ . This principle asserts that the probability of receiving a positive outcome should be the same for all demographic groups, regardless of their true label. This principle is formally expressed as:

$$P(\hat{y} = 1|s = 0) = P(\hat{y} = 1|s = 1) \quad (13)$$

In practice, we measure the violation of this metric by calculating the absolute difference in positive prediction rates between groups, known as the DP Difference ( $\Delta_{DP}$ ). A smaller value indicates a fairer model.

$$\Delta_{DP} = |P(\hat{y} = 1|s = 0) - P(\hat{y} = 1|s = 1)| \quad (14)$$

#### B.1.2 EQUAL OPPORTUNITY (EO)

Equal Opportunity imposes a more targeted requirement: for nodes that genuinely belong to the positive class ( $y = 1$ ), the model’s prediction  $\hat{y}$  should be conditionally independent of the sensitive attribute  $s$ . In other words, this ensures that individuals who are truly positive have an equal chance of being correctly identified, regardless of their group membership.

This is equivalent to requiring that the True Positive Rate (TPR) be consistent across different groups, which is formally defined as:

$$P(\hat{y} = 1|s = 0, y = 1) = P(\hat{y} = 1|s = 1, y = 1) \quad (15)$$

Similarly, we quantify the violation of this metric by calculating the absolute difference in the True Positive Rates between groups, referred to as the EO Difference ( $\Delta_{EO}$ ). A value closer to zero signifies better performance in terms of equal opportunity.

$$\Delta_{EO} = |P(\hat{y} = 1 | s = 0, y = 1) - P(\hat{y} = 1 | s = 1, y = 1)| \quad (16)$$

864 B.2 MULTI-VIEW INFORMATION BOTTLENECK  
865

866 In case of dealing with complex information systems like graph data  $\mathcal{G}$ , a single  
867 source of information is often insufficient to capture the full spectrum of factors  
868 required for decision-making. The predicted label of a node is typically influenced  
869 by multiple information sources, or views, such as its intrinsic attributes  $\mathbf{X}$ , topo-  
870 logical structure  $\mathbf{A}$ , and even global information diffusion patterns. The traditional  
871 single-view IB Kawaguchi et al. (2023)theory provides a core principle for under-  
872 standing the trade-off between accuracy and compression. Its objective is to derive  
873 an optimal representation  $\mathbf{Z}$ , by maximizing the mutual information between the  
874 target labels  $Y$  and the representation  $\mathbf{Z}$ , while simultaneously minimizing the mu-  
875 tual information between an input (e.g.,  $\mathbf{X}$ ) and the representation  $\mathbf{Z}$ . However,  
876 when information originates from multiple heterogeneous views  $\{\mathcal{G}_1, \mathcal{G}_2, \dots, \mathcal{G}_V\}$ ,  
877 a more powerful theoretical tool is needed to guide the learning process.  
878

880 To this end, we introduce and extend the Multi-view Information Bottleneck  
881 (MIB) Chaudhuri et al. (2009) principle. The core idea of MIB is to learn a fused  
882 and compact representation matrix  $\mathbf{Z}$ , from multiple information views. This rep-  
883 resentation must satisfy two primary objectives:  
884

- 885 • **Maximize Compression:** The representation  $\mathbf{Z}$  must maximally compress  
886 the total information from all views to filter out task-irrelevant redundancy  
887 and noise.  
888
- 889 • **Maximize Relevance:** Simultaneously,  $\mathbf{Z}$  must preserve the most sufficient  
890 information relevant to the downstream prediction task (represented by the  
891 labels  $Y$ ) to ensure the model’s predictive performance.  
892

894 C METHODOLOGY  
895

896 After constructing the three disentangled views, our objective is to learn a fair and  
897 compressed representation. To this end, we adapt and extend the principles of the  
898 CFB Gálvez et al. (2021). The core objective is to learn a mapping from a graph  
899 view  $\mathcal{G}_{\text{view}}$  to a latent representation  $\mathbf{Z}_{\text{view}}$ . This mapping aims to minimize the  
900 information from  $\mathcal{G}_{\text{view}}$  contained in  $\mathbf{Z}_{\text{view}}$  while maximizing the task-relevant infor-  
901 mation for  $Y$  that is independent of the sensitive attribute  $\mathbf{S}$ .  
902

903 For our Multi-view model, the total optimization objective can be written in the  
904 following Lagrangian form:  
905

$$906 \min_{P(\mathbf{Z}|\{\mathcal{G}_{\text{view}}\})} \{I(\mathbf{S}; \mathbf{Z}) + I(\{\mathcal{G}_{\text{view}}\}; \mathbf{Z}|\mathbf{S}, Y) - \beta I(Y; \mathbf{Z}|\mathbf{S})\} \quad (17)$$

907 where  $\mathbf{Z}$  is the final representation fused from the three view-specific representa-  
908 tions:  $\mathbf{Z}_{\text{feat}}$ ,  $\mathbf{Z}_{\text{struct}}$ , and  $\mathbf{Z}_{\text{diff}}$ . Based on information-theoretic properties and the  
909 Markov chain assumption  $(\mathbf{S}, Y) \leftrightarrow \{\mathcal{G}_{\text{view}}\} \rightarrow \mathbf{Z}$ , this objective can be simplified  
910 to:  
911

$$912 \min_{P(\mathbf{Z}|\{\mathcal{G}_{\text{view}}\})} \{I(\{\mathcal{G}_{\text{view}}\}; \mathbf{Z}) - \gamma I(Y; \mathbf{Z}|\mathbf{S})\}, \quad \text{where } \gamma = \beta + 1 \quad (18)$$

913 This formulation intuitively expresses our dual objectives: (1) Compression: min-  
914 imizing the total information  $I(\{\mathcal{G}_{\text{view}}\}; \mathbf{Z})$  extracted from all views; and (2) Fair  
915

918 Prediction: maximizing the task-relevant information  $I(Y; \mathbf{Z}|\mathbf{S})$  contained in the  
 919 representation  $\mathbf{Z}$ , conditioned on the sensitive attribute  $\mathbf{S}$ .  
 920

921 As illustrated in the overall framework, each view  $\mathcal{G}_{\text{view}}$  is processed by an indepen-  
 922 dent variational graph encoder  $g_{\theta_{\text{view}}}$  Kipf & Welling (2016). The encoder outputs  
 923 the parameters of the latent distribution for each node, namely the mean vector  
 924  $\mu_{\text{view}}$  and the log-variance vector  $\log \sigma_{\text{view}}$ . We utilize the reparameterization trick  
 925 to sample from this distribution, which ensures that gradients can be backpropa-  
 926 gulated through the sampling process:  
 927

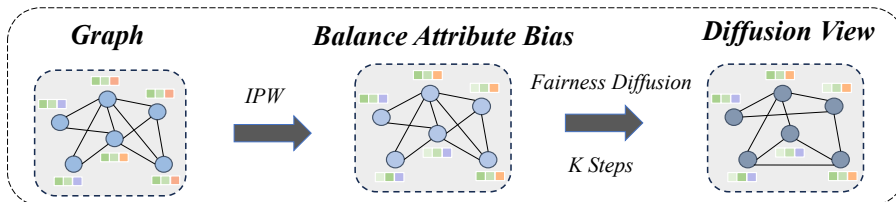
$$\mathbf{Z}_{\text{view}} = \mu_{\text{view}} + \sigma_{\text{view}} \odot \epsilon, \quad \text{where } \epsilon \sim \mathcal{N}(0, \mathbf{I}) \quad (19)$$

930 After obtaining the latent representations for the three views, we perform an initial  
 931 fusion via element-wise addition. The result is then passed through a projector  
 932 layer, implemented as a Multi-Layer Perceptron (MLP), to learn more complex  
 933 interactions and to generate the final unified representation,  $\mathbf{Z}_{\text{proj}}$ :  
 934

$$\mathbf{Z}_{\text{proj}} = \text{Projector}(\mathbf{Z}_{\text{feat}}, \mathbf{Z}_{\text{struct}}, \mathbf{Z}_{\text{diff}}) \quad (20)$$

### 938 C.1 BALANCE DIFFSSION VIEW

940 Diffusion Views help us to identify potential dynamic deviations that may occur as  
 941 information propagates across a graph. To prevent sensitive attributes from becom-  
 942 ing biased during diffusion, we have implemented proactive intervention measures  
 943 to balance this bias, as shown in the Figure 5.  
 944



953 Figure 5: The generation process for the Diffusion View begins with the original attributed graph.  
 954 First, attribute bias is balanced using Inverse Propensity Weighting (IPW). A K-step fairness diffu-  
 955 sion process is then executed on this basis to ultimately generate the Diffusion View, which incor-  
 956 porates fair neighborhood information.  
 957  
 958

## 959 D EXPERIMENTS

### 960 D.1 BASELINE

963 The methods under discussion can be categorized as follows: FairGNN Dai &  
 964 Wang (2021) and FairVGNN Wang et al. (2022) belong to the class of adversar-  
 965 ial representation learning methods; NIFTY Agarwal et al. (2021), EDITS Dong  
 966 et al. (2022), and FairGB Li et al. (2024b) are data augmentation-based methods;  
 967 GRAFair Zhang et al. (2025) is an information bottleneck-based method; and DAB-  
 968 GNN Lee et al. (2025) is a disentangled representation learning approach. For spe-  
 969 cific details, please refer to the appendix. The following is a detailed introduction  
 970 to all baseline methods.  
 971

- **FairGNN:** FairGNN Dai & Wang (2021) is a framework designed to eliminate discrimination in GNNs by using adversarial learning and a sensitive attribute estimator to achieve fair node classification even with limited sensitive attribute information.
- **NIFTY:** NIFTY Agarwal et al. (2021) is a unified approach that promotes fairness and stability in GNN representations by leveraging counterfactual perturbations and layer-wise weight normalization to ensure robust and unbiased graph embeddings.
- **EDITS:** EDITS Dong et al. (2022) mitigates bias in attributed networks for GNNs by optimizing attribute re-weighting and structural adjustments to reduce disparities between demographic groups while preserving downstream task performance.
- **FairVGNN:** FairVGNN Wang et al. (2022) is a framework that integrates adversarial learning with weight clipping to mitigate sensitive attribute leakage.
- **FairGB:** FairGB Li et al. (2024b) addresses unfairness in GNNs through group re-balancing techniques, such as counterfactual node mixup and contribution alignment, to ensure balanced influence from different demographic groups during training.
- **GRAFair:** GRAFair Zhang et al. (2025) is a variational graph auto-encoder-based framework that achieves stable fairness by minimizing sensitive information in representations via a conditional fairness bottleneck, balancing utility and debiasing without adversarial methods.
- **DAB-GNN:** DAB-GNN Lee et al. (2025) promotes fair GNN representations by disentangling and amplifying attribute, structure, and potential biases, then debiasing them to minimize subgroup distribution differences.

## D.2 ABLATION STUDY

we conducted a series of ablation studies. Our proposed framework is fundamentally an implementation of the Multi-view conditional information bottleneck, which aims to maximize task-relevant fair information while minimizing irrelevant information from the Multi-view inputs. To systematically evaluate the contribution of each core component, we constructed three key variants: FairMIB w/o m (without information compression), FairMIB w/o s (without the conditional constraint of the bottleneck), and FairMIB w/o c (without the Multi-view consistency constraint).

First, we validate the role of the conditional information bottleneck’s core mechanism by removing it (FairMIB w/o s). The objective of this component is to maximize the information in the representation that is relevant to the task  $\mathbf{Y}$  but independent of the sensitive attribute  $\mathbf{S}$ , i.e.,  $I(\mathbf{Y}; \mathbf{Z}|\mathbf{S})$ . As shown in Table 3, removing this module leads to a significant decline in model fairness. Across all datasets, the fairness metrics of FairMIB w/o s worsened significantly; for instance, on the Bail dataset, its DP metric worsening by over 30%. This indicates that conditioning the decoder on the sensitive attribute during training is crucial for compelling the

1026 encoder to learn a truly fair representation, as it effectively weakens the model’s  
 1027 ability to capture and rely on sensitive information, thereby ensuring the achieve-  
 1028 ment of the fairness objective.  
 1029

1030 Second, we investigate the contribution of information compression using the Fair-  
 1031 MIB w/o m variant. This module corresponds to the objective of minimizing mu-  
 1032 tual information between input views and the representation,  $I(\{\mathcal{G}_{\text{view}}\}; \mathbf{Z})$ , and is  
 1033 designed to prevent the model from learning redundant or harmful biased infor-  
 1034 mation. The results show that removing this module leads to a substantial decline in  
 1035 both predictive performance and fairness. This phenomenon was particularly pro-  
 1036 nounced in the Pokec-z dataset, where the DP metric increased from being nearly  
 1037 40%, and the utility also decreased. This demonstrates that the compression of re-  
 1038 dundant information effectively improves both utility and fairness by forcing the  
 1039 model to learn a compact representation, thereby filtering out bias-propagating in-  
 1040 formation from the input views.  
 1041

1042 Finally, we assess the role of the Multi-view consistency constraint by evaluating  
 1043 the FairMIB w/o c variant. The removal of this constraint leads to a noticeable  
 1044 decline in fairness performance across datasets, with the effect being particularly  
 1045 severe on the Pokec-n dataset, where both DP and EO metrics deteriorate beyond  
 1046 those observed in other ablation variants (Table 3). These results underscore the  
 1047 importance of enforcing semantic alignment between representations of different  
 1048 views through contrastive learning. By aligning the latent spaces across views, the  
 1049 model is guided to learn a robust and coherent shared representation, preventing in-  
 1050 dividual view encoders from independently capturing conflicting or biased patterns.  
 1051 This alignment is critical for the overall debiasing process, ensuring that the learned  
 1052 representations are both fair and consistent.  
 1053

1054 The above ablation study results validate the effectiveness of the three core com-  
 1055 ponents of the FairMIB model: the conditional information bottleneck, information  
 1056 compression, and the Multi-view consistency constraint. These components work  
 1057 synergistically through their respective mechanisms, collectively mitigating sensi-  
 1058 tive attribute bias by ensuring fairness objectives, filtering out irrelevant infor-  
 1059 mation, and aligning Multi-view representations.  
 1060

### 1061 D.3 MULTI-VIEW ANALYSIS

1062 To address RQ3, we conducted a series of ablation experiments to assess the con-  
 1063 tribution of each view by selectively removing the Diffusion View (w/o Diffusion  
 1064 View), the Feature View (w/o Feature View), or the Structural View (w/o Struc-  
 1065 tural View). The results presented in Table 4 indicate that the three views provide  
 1066 complementary information, and their joint utilization is critical for achieving an  
 1067 optimal balance between utility and fairness. Removing any single view typically  
 1068 results in a significant decline in model performance. For example, on the Bail  
 1069 dataset, excluding the Feature View leads to a drop of over 10% in F1-score, while  
 1070 fairness metrics DP and EO also deteriorate sharply, highlighting the essential role  
 1071 of original node attributes in maintaining both baseline predictive performance and  
 1072 fair decision-making.  
 1073

Table 3: Results of FairMIB ablations on five datasets

Datasets	Method	Acc ( $\uparrow$ )	F1-score ( $\uparrow$ )	AUC ( $\uparrow$ )	$\Delta DP$ ( $\downarrow$ )	$\Delta EO$ ( $\downarrow$ )
german	FairMIB w/o m	$70.00 \pm 0.00$	$82.35 \pm 0.00$	$60.62 \pm 4.78$	$0.51 \pm 0.02$	$0.44 \pm 0.02$
	FairMIB w/o s	$70.00 \pm 0.00$	$82.35 \pm 0.00$	$55.85 \pm 2.60$	$0.87 \pm 0.22$	$0.63 \pm 0.11$
	FairMIB w/o c	$70.00 \pm 0.00$	$82.35 \pm 0.00$	$59.25 \pm 4.25$	$0.42 \pm 0.12$	$0.55 \pm 0.01$
	FairMIB	<b><math>70.24 \pm 0.48</math></b>	<b><math>82.45 \pm 0.20</math></b>	<b><math>65.55 \pm 1.61</math></b>	<b><math>0.38 \pm 0.76</math></b>	<b><math>0.17 \pm 0.34</math></b>
bail	FairMIB w/o m	$84.32 \pm 1.34$	$77.65 \pm 1.94$	$87.76 \pm 1.55$	<b><math>0.96 \pm 0.58</math></b>	$1.83 \pm 1.44$
	FairMIB w/o s	$84.12 \pm 3.20$	$77.97 \pm 4.11$	$87.93 \pm 3.16$	$1.60 \pm 0.36$	$1.52 \pm 0.81$
	FairMIB w/o c	$84.21 \pm 3.05$	$78.11 \pm 3.83$	$88.08 \pm 2.47$	$1.34 \pm 1.25$	$1.55 \pm 0.42$
	FairMIB	<b><math>85.62 \pm 0.81</math></b>	<b><math>80.10 \pm 1.25</math></b>	<b><math>89.18 \pm 2.15</math></b>	$1.23 \pm 0.49$	<b><math>1.17 \pm 0.45</math></b>
credit	FairMIB w/o m	$78.04 \pm 0.63$	$87.51 \pm 0.10$	$71.04 \pm 1.03$	$1.27 \pm 1.70$	$0.74 \pm 1.00$
	FairMIB w/o s	$77.92 \pm 0.06$	$87.57 \pm 0.02$	$71.34 \pm 0.90$	$0.70 \pm 0.33$	$0.66 \pm 0.21$
	FairMIB w/o c	$78.07 \pm 0.29$	$87.59 \pm 0.14$	$71.62 \pm 0.97$	$0.62 \pm 0.55$	$0.28 \pm 0.31$
	FairMIB	<b><math>78.57 \pm 0.86</math></b>	<b><math>87.79 \pm 0.27</math></b>	<b><math>73.21 \pm 0.51</math></b>	<b><math>0.40 \pm 0.69</math></b>	<b><math>0.24 \pm 0.48</math></b>
Pokec-z	FairMIB w/o m	$65.70 \pm 1.85$	$67.54 \pm 0.84$	$73.11 \pm 0.89$	$3.41 \pm 2.43$	$2.90 \pm 1.42$
	FairMIB w/o s	$64.54 \pm 2.00$	$68.24 \pm 0.90$	$72.10 \pm 1.24$	$2.56 \pm 1.44$	$1.38 \pm 0.96$
	FairMIB w/o c	<b><math>66.56 \pm 1.94</math></b>	<b><math>69.04 \pm 3.45</math></b>	<b><math>74.68 \pm 1.81</math></b>	$1.43 \pm 0.67$	$2.14 \pm 1.57$
	FairMIB	$66.16 \pm 1.43$	$68.86 \pm 1.40$	$73.15 \pm 1.64$	<b><math>0.69 \pm 0.26</math></b>	<b><math>0.52 \pm 0.38</math></b>
Pokec-n	FairMIB w/o m	$65.40 \pm 1.72$	$67.33 \pm 1.58$	$72.72 \pm 2.04$	$2.04 \pm 1.17$	$1.90 \pm 1.26$
	FairMIB w/o s	<b><math>66.96 \pm 2.25</math></b>	$62.75 \pm 2.73$	$73.36 \pm 1.94$	$1.98 \pm 0.41$	$2.29 \pm 1.16$
	FairMIB w/o c	$66.48 \pm 5.14$	$67.58 \pm 1.07$	<b><math>74.21 \pm 3.80</math></b>	$2.73 \pm 1.22$	$2.80 \pm 1.74$
	FairMIB	$66.22 \pm 1.09$	<b><math>69.02 \pm 1.91</math></b>	$73.28 \pm 1.02$	<b><math>1.12 \pm 0.76</math></b>	<b><math>0.92 \pm 0.90</math></b>

Interestingly, the relative importance of the Structural and Diffusion Views varies across datasets. On the Pokec-z and Pokec-n social network datasets, which have authentic topological structures, removing the Structural View results in catastrophic performance degradation, with DP increasing by over 380% and 205%, respectively. This indicates that, in these topologies, the primary source of bias originates from the graph structure itself, making it crucial to model and debias structural information directly. Conversely, in the Credit dataset, removing the Diffusion View has the most pronounced negative effect on fairness, with DP rising by 205%. This suggests that, in this context, bias predominantly propagates through multi-hop connections, underscoring the critical role of our designed Diffusion View in capturing and correcting such biases.

Overall, these findings demonstrate that no single view universally dominates across all datasets, as the sources of bias differ depending on the graph type. This further validates the necessity and effectiveness of our Multi-view decoupling framework.

#### D.4 HYPER-PARAMETER SENSITIVITY ANALYSIS



Figure 6: Parameter sensitivity results on two datasets.

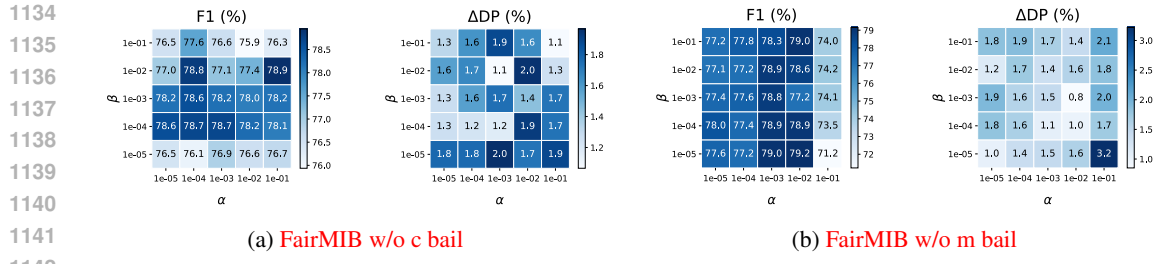


Figure 7: Parameter sensitivity results on two variants.

Table 4: Ablation over multiple views.

Datasets	Method	Acc ( $\uparrow$ )	F1-score ( $\uparrow$ )	AUC ( $\uparrow$ )	$\Delta DP$ ( $\downarrow$ )	$\Delta EO$ ( $\downarrow$ )
german	w/o Diffusion View	$70.16 \pm 0.20$	$82.35 \pm 0.03$	$57.31 \pm 4.01$	$0.51 \pm 0.92$	$0.36 \pm 0.66$
	w/o Feature View	$70.00 \pm 0.00$	$82.35 \pm 0.00$	$53.40 \pm 3.41$	$0.50 \pm 0.11$	$0.20 \pm 0.01$
	w/o Structure View	$70.00 \pm 0.00$	$82.35 \pm 0.00$	$63.07 \pm 3.69$	$0.03 \pm 0.01$	$0.02 \pm 0.03$
	FairMIB	$70.24 \pm 0.48$	$82.45 \pm 0.20$	$65.55 \pm 1.61$	$0.38 \pm 0.76$	$0.17 \pm 0.34$
bail	w/o Diffusion View	$86.19 \pm 2.53$	$80.69 \pm 3.30$	$89.44 \pm 1.85$	$1.12 \pm 0.68$	$3.22 \pm 3.14$
	w/o Feature View	$83.21 \pm 5.40$	$72.53 \pm 14.73$	$87.13 \pm 2.98$	$2.61 \pm 1.74$	$2.38 \pm 1.81$
	w/o Structure View	$83.76 \pm 1.49$	$86.79 \pm 1.65$	$86.50 \pm 1.30$	$0.79 \pm 1.18$	$0.93 \pm 1.19$
	FairMIB	$85.62 \pm 0.81$	$80.10 \pm 1.25$	$89.18 \pm 2.15$	$1.23 \pm 0.49$	$1.17 \pm 0.45$
credit	w/o Diffusion View	$78.11 \pm 0.48$	$87.53 \pm 0.06$	$69.29 \pm 2.20$	$1.22 \pm 2.39$	$0.73 \pm 1.44$
	w/o Feature View	$78.46 \pm 0.78$	$87.70 \pm 0.28$	$71.84 \pm 0.95$	$0.55 \pm 0.34$	$0.56 \pm 0.36$
	w/o Structure View	$78.94 \pm 0.88$	$87.87 \pm 0.24$	$72.19 \pm 0.93$	$1.17 \pm 0.56$	$0.70 \pm 0.44$
	FairMIB	$78.57 \pm 0.86$	$87.79 \pm 0.27$	$73.21 \pm 0.51$	$0.40 \pm 0.69$	$0.24 \pm 0.48$
Pokec-z	w/o Diffusion View	$62.19 \pm 4.16$	$69.03 \pm 1.79$	$71.90 \pm 1.59$	$1.19 \pm 0.96$	$1.62 \pm 1.53$
	w/o Feature View	$67.57 \pm 1.86$	$67.48 \pm 2.90$	$73.03 \pm 1.43$	$1.37 \pm 0.79$	$2.34 \pm 2.00$
	w/o Structure View	$65.74 \pm 3.37$	$70.78 \pm 1.15$	$75.17 \pm 3.02$	$3.33 \pm 1.09$	$1.24 \pm 0.65$
	FairMIB	$66.16 \pm 1.43$	$68.86 \pm 1.40$	$73.15 \pm 1.64$	$0.69 \pm 0.26$	$0.52 \pm 0.38$
Pokec-n	w/o Diffusion View	$65.51 \pm 0.70$	$66.05 \pm 0.62$	$71.68 \pm 0.85$	$1.29 \pm 0.89$	$1.54 \pm 1.48$
	w/o Feature View	$68.58 \pm 0.85$	$67.96 \pm 3.21$	$71.36 \pm 1.30$	$1.61 \pm 1.22$	$2.18 \pm 1.69$
	w/o Structure View	$67.15 \pm 2.42$	$66.39 \pm 0.77$	$73.83 \pm 2.84$	$3.42 \pm 2.78$	$2.75 \pm 2.57$
	FairMIB	$66.22 \pm 1.09$	$69.02 \pm 1.91$	$73.28 \pm 1.02$	$1.12 \pm 0.76$	$0.92 \pm 0.90$

We conduct a sensitivity analysis of FairMIB with respect to two hyperparameters,  $\alpha$  and  $\beta$ . In FairMIB, these hyperparameters regulate the relative contributions of information compression and view alignment. Specifically, we vary the values of  $\alpha$  and  $\beta$  within  $\{10^{-1}, 10^{-2}, 10^{-3}, 10^{-4}, 10^{-5}\}$  on the bail, Credit, Pokec-z, and Pokec-n datasets. The results of this analysis are presented in Figure 6. Overall, the performance of FairMIB remains relatively stable across a broad range of  $\alpha$  and  $\beta$ . Nevertheless, when  $\alpha$  and  $\beta$  are set to excessively large values, performance degradation may occur due to over-compression of information and overly strict view alignment. These findings highlight the necessity of balancing the two components and suggest that selecting  $\alpha$  and  $\beta$  from the range of  $10^{-3}$  to  $10^{-5}$  offers a preferable trade-off between utility and fairness. In Figure 7, we performed a hyperparameter analysis on the two variants for bail to ensure that the hyperparameters do not affect the ablation experiments.

## E USE OF LLMs

Yes, to aid or polish writing. Details are described in the paper.